

Electron impact partial ionization cross sections: R-carvone, 2-butanol, imidazole, and 2-nitroimidazole

Suriyaprasanth Shanmugasundaram  and Dhanoj Gupta* 

*Department of Physics, School of Advanced Sciences,
Vellore Institute of Technology, Katpadi,
Vellore - 632014, Tamil Nadu, India.*

Rounak Agrawal

*School of Computer Science and Engineering,
Vellore Institute of Technology, Katpadi,
Vellore - 632014, Tamil Nadu, India.*

(*dhanoj.gupta@vit.ac.in)

(Dated: December 25, 2023)

We theoretically calculate the electron impact partial and total ionization cross sections of R-carvone ($C_{10}H_{14}O$), 2-butanol ($C_4H_{10}O$), imidazole ($C_3H_4N_2$) and 2-nitroimidazole ($C_3H_3N_3O_2$). We have used the Binary Encounter Bethe (BEB) model to obtain the total electron impact ionization cross sections (TICS). The modified BEB method in combination with mass spectrum data of the molecules is used to calculate the PICS of the cationic fragments dissociating from the parent molecule. Our PICS data for R-carvone and 2-butanol are in good agreement with the experimental data for all the cation fragments along with the TICS data. For imidazole and 2-nitroimidazole, the estimates of the PICS are reported for the first time in the present study. We have found that both the modified BEB method and the mass spectrum dependence method work effectively to estimate PICS if we have information about the appearance energies and relative abundance data of the target under investigation.

I. INTRODUCTION:

Electron impact total ionization cross section (TICS) and partial ionization cross section (PICS) are important to many branches of sciences ranging from plasma physics to astrophysics and biological sciences [1–3]. In medical sciences, radiation damage to DNA/RNA is a major concern, where it has been found that secondary electrons play a crucial role in single and double-strand breaks of DNA/RNA [3, 4]. The electron impact cross sections data at low and intermediate energy are important inputs in Monte Carlo track (MCT) analysis, which is used to study damage to living cells using ionizing radiation [3]. In recent times, electron collision with biomolecules has geared up and many studies have been conducted both experimentally [5, 6] and theoretically [7–11] to provide more data for understanding the mechanism of damages caused due to the electrons. While performing the MCT simulations, only the single channel ionization is taken into account and the channels due to the dissociative ionization processes are not considered in the model, which may reduce the accuracy of the MCT analysis. Hence, the inclusion of dissociative ionization processes is important and will help us to make the MCT model more accurate. Hence, providing information on the PICS for the cations that are different due to their mass-to-charge ratio originating from their parent molecule is inevitable for accurate analysis [6]. Even with the rapid surge of electron-molecule interaction studies, there are many important molecules for which data are scarce in the literature both experimental and theoretical. In the present study, we have investigated the PICS and TICS of R-

carvone, 2-butanol, imidazole, and 2-nitroimidazole. Our motivation has been to provide the theoretical estimates of the PICS for all the cation fragments originating from the parent molecules using the recently developed methods [12, 13]. Here we will highlight the importance and applications of each of these targets.

R-carvone is an organic molecule that belongs to the class of terpenoids and has a wide variety of applications in the food industry, agriculture, and pest control. R-carvone has a minty flavored odor, used in essential oils. A recent study has found this compound can be used in anti-fungal wrapper [14, 15] for packaging fruits which increases shelf life. Jones *et al.* performed an experimental and theoretical study on electron (e,2e) impact ionization dynamics on R-carvone and its enantiomer S-carvone [16], using three-body distorted wave (3BDW) formalism for calculating the cross sections theoretically. There is a three-part study performed on this molecule by Lopes *et al.* [17] and Amorim *et al.* [18, 19]. In the first part, Lopes *et al.* [17] presented the appearance energies for 35 cations and the electron impact mass spectrum in which they observed 103 peaks with the incident electron energy of 70 eV at the mass range of 1 amu till 151 amu and compared their findings with the data available at National Institute of Standards and Technology (NIST) web book [20] and Spectral database for organic compounds (SDBS) [21]. Also, they have provided the scheme for the ionic fragmentation pathways. The successive work of Amorim *et al.* [18] presents the PICS for 78 cations from ionization threshold to 100 eV, the PICS of the isotopologue was also measured. The absolute values of PICS for all the cations presented are in the range

of 8 eV to 100 eV, only singly ionized fragments were assessed. The last work from Amorim *et al.*[19] in this series of articles contains the experimental TICS of the R-carvone compared with literature data along with the theoretically predicted TICS, using the Binary encounter Bethe (BEB) [19] model and the independent atom model (IAM) in conjunction with the screening correction additive rule (SCAR) incorporating the interference effects (I) also, which is colloquially called IAM+SCAR+I method which can be used to calculate the TICS [22–26]. In all the studies, Lopes *et al.*, used Hiden analytical energy pulse ion counting (EPIC) quadrupole mass spectrometer (QMS - EPIC 300) which can detect mass from 1 amu to 300 amu comprising a detector resolution of 1 amu which was used at residual gas analyzing (RGA) mode.

2-butanol is a colorless organic solvent that also possesses chirality [27]. Recently the compound has become a study of interest for many researchers as it can be a potential replacement for gasoline and can be directly used as a replacement without modifying the engines [28] and references therein. Like other alcohols 2-butanol also belongs to the class of biofuels like methanol, ethanol, 1-propanol, and 1-butanol. Several experimental and theoretical investigations are available for these molecules [13, 29, 30] and references therein. Nirali *et al.*[31] provided a recent study of electron collision dynamics with n-butanol containing an extensive review of the available literature on n-butanol. But studies on 2-butanol are scarce. Researchers are looking to engineer microbes to produce fuels such as 1-butanol and 2-butanol and have identified an engineered strain of *L. diolivorans* microbe, which can be used to produce 2-butanol up to 10g/Litre from meso-2,3-butanediol through an anaerobic fermentation process [32]. Amorim *et al.*[33] experimentally observed the mass spectrum for 51 cations and the appearance energies for 38 cationic fragments of 2-butanol are provided in their work. For their measurements, they used the same QMS EPIC - 300 operated on residual gas analyzing (RGA) mode [17, 29, 34]. Lopes *et al.* have performed a comprehensive review on the fragmentation of biofuels which contains all the literature till the year 2019 for the methanol, ethanol, propanol, and butanol molecules [28]. Bettega and co-workers performed low-energy electron scattering studies on isomers of butanol including 2-butanol where they presented the differential

cross sections (DCS), momentum transfer cross sections (MTCS), and integral cross sections (ICS) for an incident energy range of 1 eV to 50 eV [35]. The preceding work of Amorim *et al.* provided the experimental PICS for the fragments of 2-butanol along with their experimental TICS and theoretical TICS using the BEB method and the IAM+SCAR+I method [36].

imidazole acts as a base for several biomolecules. imidazole and 2-nitroimidazole are very good radiosensitizers used in cancer treatment and also in the development of drugs in pharmaceutical chemistry [37]. A brief review [38, 39] of their use provides us with the importance of these targets for various applications. Rebecca *et al.*[40] studied the low-energy fragmentation of imidazole and 2-nitroimidazole, and has provided us with the appearance energies and mass spectrum for the cationic fragments. A recent study by Tejas *et al.*[41] for imidazole has investigated the dissociative electron attachment (DEA), excitation, and ionization processes by electron impact.

In the present study, we have made use of the appearance energies and mass spectrum data from the literature [17, 33, 40] for all the targets studied here. The structure of the article is as follows: In section II, we have discussed the BEB model for TICS and the computational method to calculate orbital energies required as input in the BEB model. In sections ??, various methods to calculate the PICS using the BEB model, appearance energies, and mass spectrum data are discussed. In section III, we have shown the results and their discussions. In Section IV we summarize our results and findings.

II. BEB MODEL

The BEB model [42] is one of the most common and widely used methods for predicting the TICS for atoms, molecules, radicals, and ions and is being employed here with some modifications to calculate the PICS. The BEB method calculates the electron impact ionization cross section for each orbital and the sum of the ionization cross section for each orbital gives the total ionization cross section [Eq. (1)] for a target under consideration. [Eq (2)] gives the BEB formula for determining the TICS.

$$\sigma_{TICS}(E) = \sum_i^N \sigma_i(E) \quad (1)$$

$$\sigma_i^{BEB}(E) = \frac{S}{(t_i + u_i + 1)/n} \left[\frac{Q_i \ln t_i}{2} \left(1 - \frac{1}{t_i^2} \right) + (2 - Q_i) \left\{ \left(1 - \frac{1}{t_i} \right) - \frac{\ln t_i}{t_i + 1} \right\} \right] \quad (2)$$

The reduced variables t_i, u_i and S are defined,

$$S = 4\pi a_0^2 N \left(\frac{R}{B} \right)^2, \quad u_i = \frac{U}{B}, \quad t_i = \frac{E}{B}, \quad Q_i = 1 \quad (3)$$

Here, (n) is the principal quantum number, $(a_0 = 0.52918 \text{ \AA})$ is the Bohr radius, $(R = 13.6057 \text{ eV})$ is Rydberg constant, (B) is the occupation number of the

orbitals, (U) is the orbital kinetic energies, (N) is the orbital occupation number, (E) is the incident electron kinetic energy and (Q_i) is differential oscillator strength which is set to unity according to the simplified BEB model.

To calculate the orbital parameters that are required as input to the BEB model we adopted the similar methodology that was applied in our recent work [43], we first optimized the target molecules using the density functional $\omega B97X - D$ with the aug-cc-PVTZ (aVTZ) basis set, which calculates the energy minima at which the molecule is more stable. After optimization, the orbital binding and kinetic energies are calculated using the Hatree-Fock (HF) approximation that has been found to work efficiently over the years within 10 % \sim 15 % of experimental uncertainty[44]. All the quantum chemistry calculations are performed using the Gaussian-16 [45] quantum chemistry software. The structures of the target molecules studied are shown in Figure. 1. The main aspect of this work is to calculate the branching ratios and PICS of the possible fragments forming from the parent molecules which is described in the sections to follow.

A. Branching ratio (BR) and Partial ionization cross section (PICS)

When the molecular target undergoes dissociative ionization (DI) by an electron or positron impact, there will be several reaction channels in which DI takes place. The electron impact mass spectrum (EIMS) is a characteri-

zation technique that can provide information about the various cations present, along with their mass-to-charge ratio (m/z), relative abundances, and respective appearance energies. Here, the branching ratio plays an important role, which describes the contribution of each reaction channel to the TICS. There are different methods proposed to calculate the branching ratio (BR), which in turn is used to compute the PICS. Karl Irikura [46] used the EIMS data from the NIST [20] to calculate BR and have used that to compute the PICS of many organic molecules at a single electron impact energy. Hamilton *et al.*[47] used the experimental EIMS to calculate the BR and hence the PICS, which is discussed in more detail later. Huber *et al.*[48] proposed the way to calculate the BR using the appearance energy of the fragments by electron impact. The BR was combined with the TICS from the BEB method to obtain the PICS for various fragments which is discussed in more detail below in Section. II B. Hamilton *et al.*[47] proposed a modification in the reduced variable $t_i = E/B$, which is given in Eq. (4).

$$t'_i = \left(\frac{E}{B - \varepsilon} \right) \quad (4)$$

Here, ε can either be the appearance energy (AE) or the dissociation energy (ε) for the specific fragment. The AE and ionization energy (IE) or ionization potential (IP) aren't the same, IP is the minimum energy that is required to remove an electron from a molecule's bound state whereas the AE is the minimum energy required to induce fragmentation of a molecule. After the modification of Eq.(4), the modified BEB formula given in Eq.(5) can be used to calculate PICS,

$$\sigma_i^{mBEB-A}(E) = \frac{S}{(t'_i + u_i + 1)/n} \left[\frac{Q_i \ln t'_i}{2} \left(1 - \frac{1}{t_i'^2} \right) + (2 - Q_i) \left\{ \left(1 - \frac{1}{t'_i} \right) - \frac{\ln t'_i}{t'_i + 1} \right\} \right] \quad (5)$$

Using Eq.(5) the PICS of each fragment can be calculated as,

$$\sigma^{PICS}(E) = \Gamma_i(E_r) \times \sigma_i^{mBEB-A}(E) \quad (6)$$

Here, $\Gamma_i(E_r)$ is the experimental BR obtained from the electron impact mass spectrometry (EIMS). The EIMS is performed at the reference incident electron energy (E_r) of 70 eV or 100 eV. The branching ratio of the fragment is defined as,

(7)

$R(E_r)$ denotes the relative intensity of the particular fragment and $T(E_r)$ is the total ion intensity which is the sum of all the relative intensity of the fragments that are detected. In case of unavailability of EIMS data for a molecule of interest, performing quantum chemical mass spectrometry (QCxMS) [49] can provide information on

the fragments along with their relative abundances and fragmentation pathways. The project QCxMS is very well tested [50] and is actively under development for more accurate prediction of the EIMS theoretically.

On the other hand Baluja *et al.*[51] presented a similar form of the Eq.(5), where they also call it a modified BEB method, we address their model with the superscript B making it σ^{mBEB-B} . The key assumption in the mBEB-B model is, that the cation that is dissociated from the neutral parent molecule can be distinguished by their ε , which is different from IE that corresponds to the neutral molecule. The vertical IE is the energy of the highest occupied molecular orbital (HOMO). To make the BEB

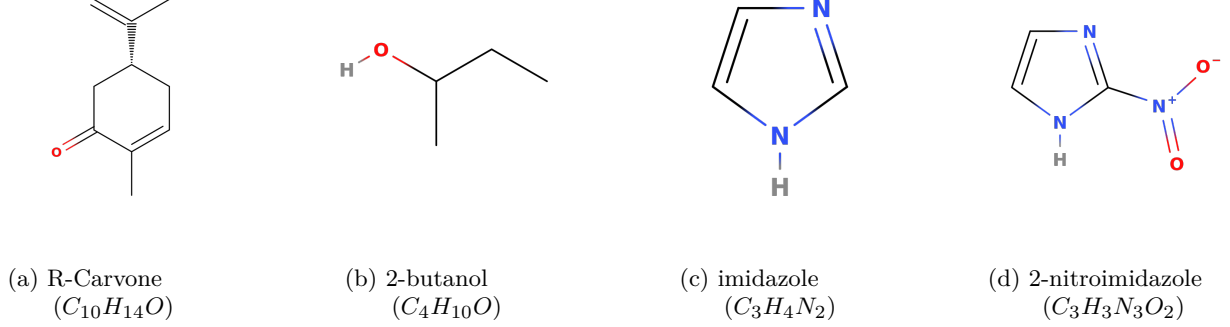


FIG. 1: Structure of molecular targets, for which the PICS were presented in this manuscript.

model feasible across cations, a consistent alteration is made in the values of occupied orbitals binding energies. The changes are accomplished by adding the difference (δ) between IE of the neutral molecule and the ε of the

cation $\delta = (IE - \varepsilon)$ to the all the values in orbital binding energy (B) of the neutral molecule ($B' = B + \delta$). As a result, the HOMO of the particular cation becomes its appearance energy.

$$\sigma_i^{mBEB-B}(E) = \frac{S^*}{(t_i^* + u_i^* + 1)/n} \left[\frac{Q_i \ln t_i^*}{2} \left(1 - \frac{1}{t_i^{*2}} \right) + (2 - Q_i) \left\{ \left(1 - \frac{1}{t_i^*} \right) - \frac{\ln t_i^*}{t_i^* + 1} \right\} \right] \quad (8)$$

The new reduced variables are,

$$S^* = 4\pi a_0^2 N \left(\frac{R}{B'} \right)^2, \quad t_i^* = \left(\frac{E}{B'} \right), \quad u_i^* = \frac{U}{B'}, \quad Q_i = 1 \quad (9)$$

The PICS is calculated using a similar approach used in Eq. (6)

$$\sigma^{PICS}(E) = \Upsilon_i(E_r) \times \sigma_i^{mBEB-B}(E) \quad (10)$$

The PICS calculated from the mBEB-B model is then scaled using the factor $\Upsilon_i(E)$, which is obtained from the experimental BR $\Gamma_i(E)$ Eq.(7) and the theoretical BR which is calculated from the PICS itself. The theoretical BR for the fragment is calculated at the same incident energy as the experimental BR $\Gamma_i(E)$,

$$\Gamma_i^{Theo}(E_r) = \frac{\sigma_i^{mBEB-B}(E_r)}{\sigma_i^{BEB}(E_r)} \quad (11)$$

There are other ways to calculate the theoretical BR without the need for PICS, which was introduced by Huber *et al.*[48] which will be explained in the later part of this article. The scaling factor $\Upsilon_i(E_r)$ is obtained by

$$\Upsilon_i(E_r) = \frac{\Gamma_i(E_r)}{\Gamma_i^{Theo}(E_r)} \quad (12)$$

This scaling factor implemented by Baluja *et al.*[51] and the structural factor incorporated by Huber *et al.*[48] and Vincent *et al.*[12] are the same, details about structural factor are discussed in the next section.

B. Huber's method

To theoretically calculate the BR of the fragments we require the information about the dissociation energies (ε). b_i is the branching factor, which isn't the same as BR.

$$b_i = \left(\frac{1}{\varepsilon} \right)^\alpha \quad \text{if } E \geq \varepsilon \quad (13)$$

α is a parameter that is used to make the b_i slowly reach the asymptotic region and if the incident energy is less than the ε then b_i is 0 as the dissociation never commences. In our case, we keep it as 3 as proposed by Huber *et al.*[48]. The theoretical BR calculated by Huber's method is given below and is denoted by the superscript H.

$$\Gamma_i^H(E_r) = \begin{cases} \frac{b_i}{\sum_i^n b_i} & \text{if } E \geq \varepsilon \\ 0 & \text{if otherwise} \end{cases} \quad (14)$$

It is provided that the additional structural factor (χ_i) paves the way for other processes within the threshold region.

$$\Gamma(E_r) = \Gamma_i^H(E_r)\chi_i(E_r) \quad (15)$$

Γ_i^H is the actual BR, and χ is determined from the experimental BR (Γ_i) by taking the ratio of experimental BR to that of theoretical BR calculated using Huber's method at the reference energy,

$$\chi_i(E_r) = \frac{\Gamma_i(E_r)}{\Gamma_i^H(E_r)} \quad (16)$$

The way this structural factor is calculated is the same as the scaling factor (Υ_i) which was discussed earlier. It is shown that for simple dissociation of $C-H$ bonds, the χ_i is taken as, $\chi_i \leq 1$ and for more complex dissociation it is suggested to be $\chi_i > 1$ [48]. It was considered $\chi_i = 1$ by Vincent *et al.*[12] for the ease of calculation of branching ratios and this could be explored further in the future.

C. Mass spectrum dependence (MSD) method

In all the above methods the BR is calculated at a single energy, this method was proposed to make the branching ratio dependent on the incident energy of the electron. The BR calculated using this method will be denoted with the superscript (MSD), continuous data for all energy ranges.

$$\Gamma_i^{MSD}(E) = \begin{cases} 0 & \text{if } E < \varepsilon \\ \Gamma_i(E_r) \left[1 - \left(\frac{\varepsilon}{E} \right)^\nu \right] & \text{if } E \geq \varepsilon \end{cases} \quad (17)$$

Here, we would also need a BR at the reference energy, which can either be theoretical BR or experimental BR. Suppose, there are no experimental EIMS data present for the target then we can use the theoretical BR calculated from Huber's method, referred to as the hybrid method by Vincent *et al.*[12]. This assumption is true only if we strictly interpret that the already computed branching ratios are asymptotic when the incident energy is infinity, the branching ratio reaches the known branching ratio which gives rise to the assumption that reference energy is at infinity. Also, this method does not give the same reference branching ratio at the reference incident energy [12]. The control parameter ν was taken as 1.5 ± 0.2 by Janev *et al.*[52], it was taken as 1.5 in this work as an average value. As we have discussed several methods to calculate the branching ratios, we should also remember that the sum of all the branching ratios of the fragments should sum up to give unity $\sum_i \Gamma_i = 1$, irrespective of the methods employed. However, this condition may not be satisfied if we do not have information on all the fragmentation or dissociation pathways for a target molecule.

III. RESULTS AND DISCUSSIONS

We have theoretically calculated the PICS for all the molecular targets which we have shown in Figure. 1 using the mBEB-B method and the MSD method. Here we did not employ Huber's method [48] and the mBEB-A [47] method as the magnitude of their cross sections was not as accurate as the MSD method [12] or the mBEB-B method [51] as compared to experimental results. More details can be found in the upcoming subsections.

A. R-Carvone

In the series of articles published by Lopes *et al.*[17] and Amorim *et al.*[18, 19] have extensively studied the fragmentation of R-carvone by electron impact and provided the absolute PICS and TICS along with the mass spectrum and appearance energies and the Wannier exponents for 35 cations. We have calculated the theoretical PICS for these fragments using the MSD method [Eq. (17)], and mBEB-B method [Eq. (8)] based on the data presented by Lopes *et al.*[17] and Amorim *et al.*[18, 19]. The most stable cations were found to have masses of 39 amu [$C_3H_3^+$], 54 amu [$C_4H_6^+$], and 82 amu [$C_5H_6O^+$], as their relative abundances contribute 40% to the total ion intensity. Owing to higher contribution in the mass spectrum, their PICS also tend to have higher magnitudes than other cations which can be seen from the Table. I. In the MSD method the BR is scaled for the incident energy whereas in the mBEB-B method, the binding energies of the molecular orbitals are scaled to the appearance energy of the cations. Although they seem different from one another, but work the same when it comes to calculating the PICS. In Table.I, we have shown all the important data that we have obtained while performing our calculations. It consists of the BR obtained using Huber's method (Γ_i^H) [Eq. (14)], theoretical BR (Γ_i^{theo}) which is calculated while performing the mBEB-B method [Eq. (11)], the experimental BR (Γ_i) which is obtained from the EIMS data presented by Lopes *et al.*[17] [Eq. (7)], the structural factor (χ_i) [Eq. (16)], the scaling factor (Υ_i) [Eq. (12)] and the PICS max from the MSD method and the mBEB-B method compared with the experimental PICS max [18]. The mBEB-B PICS presented in the table are scaled using the (Υ_i). We have also calculated the mean squared error (MSE) for the PICS, assuming that the experimental values are true values and the PICS we obtained as predicted values. The MSE for MSD-PICS was 0.1327 and the MSE for mBEB-B was 0.1038 giving almost similar PICS. In the Figure.3, It is seen that for most of the fragments, the PICS calculated using both methods shows good agreement with the experimental PICS. Some discrepancies of the present data with the experiment are seen for cations [CH_2^+], [$C_3H_3^+$], [$C_7H_6O^+$] and [$C_3H_5^+$] where our data are found to underestimate the experimental results, the reason for the discrepancy may be due to the

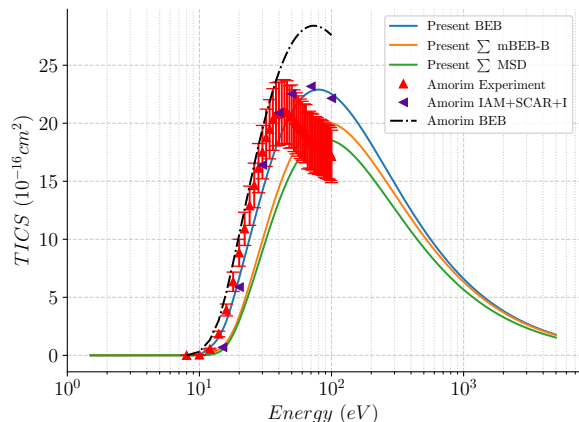


FIG. 2: Comparison of TICS of R-carvone with the literature. The blue line represents our present TICS calculated using the BEB method, the orange line represents the sum of all the PICS calculated for the various cations using the mBEB-B method, and the green line represents the PICS calculated using the MSD method. The red upright triangle represents the TICS presented by Amorim *et al.*[19], the purple left triangle represents the TICS which was calculated using IAM+SCAR+I by Amorim *et al.*[19] and the black dotted lines represents the TICS calculated using the BEB model by Amorim *et al.*[19]

appearance energies and the relative abundance which are smaller in our case compared to experimental values. Also, there were two isomers detected in the mass spectrum $[C_2H_5]^+/[CHO]^+$ and $[C_2HO]^+/[C_3H_5]^+$ which had two distinct AEs that are mentioned in square brackets in the Figure. 3. However, for a few cations like $[O]^+$, $[C_2H_2]^+$, $[C_3H_4]^+$, $[C_4H_5]^+$, the PICS calculated using the MSD shows a very good agreement with the experimental data of Amorim *et al.*[18], whereas for several other cations both the MSD method and the mBEB-B method predicts the PICS within the experimental uncertainty as shown Figure.3. In Figure. 2, shows the TICS obtained using the BEB model, MSD, and mBEB-B methods which is the sum of the PICS of all the fragments. Our results are compared with the existing experimental and theoretical data [18, 19], and the present results using the mBEB-B method are found to be in excellent agreement with the experimental data. Our TICS using the MSD method is found to underestimate all other data because the appearance energies were not provided for all the fragments. In the series of articles [17–19] they have presented the experimental PICS at 100 eV for 78 cationic fragments but have only provided the AE for 35 prominent cations. We believe if we could calculate the PICS for other remaining fragments and sum it then it might give a better comparison with the experimental TICS and the TICS calculated using the BEB model.

B. 2-butanol

The PICS that we have theoretically determined for the fragments of 2-butanol are based on the EIMS data presented by Amorim *et al.*[33], their experimentally provided EIMS, AEs for 51 cations. Pires *et al.*[29] and Gosh *et al.*[30] provided the EIMS, AEs, and the experimental PICS for the fragments of 1-butanol. Goswami *et al.*[13] have theoretically calculated the PICS using the mBEB-B method [Eq.(8)], which has good agreement with the existing experimental PICS presented by Pires *et al.*[29] and the experimental TICS presented by Gosh *et al.*[30]. Owing to a good comparison of the mBEB-B model with the literature data in 1-butanol, we proceed to calculate the PICS theoretically applying both the mBEB-B model and the MSD method that requires the experimental EIMS data. In Table. II, all the relevant data required for calculating the PICS using the mBEB-B and MSD are given similarly to R-carvone. The maximum cross sections are also provided in the table using the two methods and are compared with the experimental maximum cross section. In Figure. 5, we have compared our PICS data with the experimental PICS presented by Amorim *et al.*[36] in the entire energy range. The MSD method and mBEB-B method for 2-butanol show excellent comparison with the experimental data of Amorim *et al.*[36] for most of the cationic fragments. However, for a few fragments such as $[CH]^+$, $[C_2H_2]^+$, $[C_3H_2]^+$, and $[C_3H_3]^+$, there were slight discrepancies when comparing our data with the experimental PICS which can be seen in Figure. 5. The PICS that we calculated are consistent for all cations from their AE threshold to 5000 eV, magnitudes of the PICS of the cations differ concerning their RI and AE.

Figure. 4, shows the comparison of our TICS with the existing data available in the literature for 2-butanol. The present TICS calculated using the BEB method, compares very well with the experimental data and lies within the uncertainty of the experimental TICS. Also the TICS (obtained after summing all the PICS of the fragments) from the mBEB-B and MSD methods compare well with the experiment and are within the range of uncertainty of the experimental TICS. The average experimental uncertainty is 19% and all our present data lies within that limit.

C. imidazole (IMI) and 2-nitroimidazole (2NI)

The PICS that we present here for IMI and 2NI are based on the mass spectrum and AEs presented by Rebecca *et al.*[40]. In Table III, and Table. IV, we have presented the BRs calculated using Huber’s method [Eq.(14)], the theoretical BRs [Eq.(11)], the experimental BRs calculated from the EIMS data [Eq.(7)] and the structural factor [Eq.(16)] and the scaling factor [(12)] along with the maximum cross sections calculated using the MSD and the mBEB-B methods. The PICS for $[HCNH]^+$, $[HCCNH]^+$, $[HCNCH]^+$ and

TABLE I: Absolute values of branching ratio (Γ) structural factor (χ_i), scaling factor (Υ) and maximum PICS calculated using MSD and mBEB-B method compared with experimental PICS [18] for R-carvone

m/z	Cations ^a	ε (eV) [17]	Γ_i^H	Γ_i^{Theo}	Γ_i [17]	χ_i	Υ_i	σ_{max}^{MSD}	σ_{max}^{mBEB-B}	σ_{max}^{exp} [18]
14	CH_2	15.34	0.033333	0.540558	0.001539	0.046171	0.002847	0.03263	0.037382	0.04474
16	O	14.16	0.030769	0.608827	0.002601	0.084534	0.004271	0.055578	0.062124	0.05242
26	C_2H_2	11.67	0.025358	0.794778	0.004087	0.161172	0.005142	0.08878	0.094934	0.08685
28	C_2H_4/CO	12.3	0.026727	0.741232	0.032002	1.197369	0.043174	0.692441	0.748003	0.64644
28	C_2H_4/CO	14.58	0.031681	0.583319	0.032002	1.010126	0.054862	0.682016	0.768848	0.64644
29	C_2H_5/CHO	12.04	0.026162	0.762717	0.014356	0.548735	0.018822	0.311144	0.334674	0.37457
29	C_2H_5/CHO	14.93	0.032442	0.563107	0.014356	0.442517	0.025494	0.305212	0.346601	0.37457
31	CH_3O	11.97	0.026010	0.768646	0.000531	0.020415	0.000690	0.011508	0.012364	0.01021
39	C_3H_3	10.83	0.023533	0.874773	0.074061	3.147148	0.084663	1.617523	1.708448	2.61851
39	C_3H_3	15.61	0.033919	0.526334	0.074061	2.183447	0.140712	1.567225	1.806174	2.61851
40	C_3H_4	10.63	0.023098	0.895457	0.010667	0.461812	0.011913	0.233269	0.245712	0.2041
41	C_2HO/C_3H_5	12.56	0.027292	0.720556	0.046743	1.712707	0.06487	1.009673	1.095517	2.15466
41	C_2HO/C_3H_5	14.82	0.032203	0.569361	0.046743	1.451525	0.082097	0.994528	1.126763	2.15466
42	C_2H_2O	10.32	0.022425	0.928897	0.005758	0.256772	0.006199	0.126158	0.132352	0.11159
43	C_2H_3O	11.99	0.026053	0.766946	0.007496	0.287718	0.009774	0.162525	0.174674	0.15451
45	C_2H_5O	11.99	0.026053	0.766946	0.000756	0.029017	0.000986	0.016396	0.017622	0.01444
52	C_4H_4	10.68	0.023207	0.890223	0.005387	0.232130	0.006051	0.117758	0.124124	0.10637
53	C_4H_5	12.52	0.027205	0.723686	0.024386	0.896380	0.033697	0.526899	0.571304	0.50587
54	C_4H_6	13.81	0.030008	0.631203	0.093897	3.129061	0.148758	2.011533	2.233011	2.43499
55	C_4H_7	12.67	0.027531	0.712042	0.009911	0.359995	0.013919	0.213932	0.232561	0.19521
58	C_3H_6O	10.01	0.021751	0.964127	0.029481	1.355390	0.030578	0.647126	0.676302	0.56612
60	C_3H_8O	10.62	0.023076	0.896510	0.000836	0.036227	0.000932	0.01828	0.019252	0.01595
65	C_5H_5	15.31	0.033267	0.542169	0.006979	0.209785	0.012872	0.147989	0.169430	0.1409
67	C_5H_7	12.16	0.026423	0.867692	0.012153	0.459945	0.016146	0.263205	0.283664	0.24021
69	C_5H_9	10.94	0.023772	0.863681	0.007894	0.332075	0.00914	0.172297	0.182264	0.15821
77	C_6H_5	13.12	0.028509	0.678578	0.010561	0.370448	0.015564	0.227293	0.249071	0.2091
79	C_6H_7	11.13	0.024185	0.844976	0.016200	0.669847	0.019172	0.353152	0.374592	0.32259
80	C_5H_4O	9.63	0.020925	1.009962	0.007271	0.347475	0.007199	0.159963	0.16644	0.14366
82	C_5H_6O	10.85	0.023576	0.872742	0.132679	5.627668	0.152025	2.897386	3.061113	2.71195
83	C_5H_7O	10.9	0.023685	0.867692	0.007231	0.305301	0.008334	0.157858	0.166896	0.13467
91	C_7H_7/C_6H_3O	10.83	0.023533	0.874773	0.012047	0.511925	0.013772	0.263116	0.277906	0.23679
92	C_7H_8/C_6H_4O	9.87	0.021447	0.980661	0.00743	0.346440	0.007577	0.163231	0.170305	0.14487
93	C_6H_5O	10.83	0.023533	0.874773	0.036261	1.540875	0.041452	0.791954	0.836472	0.73009
94	C_6H_6O	9.72	0.021121	0.998829	0.007258	0.343642	0.007266	0.159585	0.166215	0.13833
106	C_7H_6O	9.56	0.020773	1.018745	0.007258	0.349394	0.007124	0.159737	0.166078	0.3352
107	C_7H_7O	9.35	0.020317	1.045762	0.01815	0.893349	0.017356	0.399984	0.414931	0.35451
108	C_7H_8O	10.2	0.022164	0.942315	0.034881	1.573783	0.037017	0.764773	0.801114	0.69171
135	$C_9H_{11}O$	10.27	0.022316	0.934455	0.003728	0.167056	0.003990	0.081708	0.085665	0.07175

^a The forward slash denotes "or" added for the cations with same m/z values

but has a different AE and $[IMI - H]^+$ is the dehydrogenated IMI which was also observed in the EIMS experiment. For fragments which has the same m/z values and AEs, the calculated PICS will be the same and is presented in one figure for both fragments. From the Figure. 6a, it can be seen that for almost all the fragments the magnitude of the PICS from the MSD method is slightly smaller than the PICS calculated using the mBEB-B method. Both methods match very well from the ionization threshold to 70 eV after which the cross sections show slight variation for all the fragments.

In Figure 6b, we have compared all the TICS from the existing literature along with our data. Our BEB TICS compares very well with the BEB TICS presented by Tejas *et al.*[41], albeit their TICS calculated using the

msp-ic method has a higher magnitude in comparison to BEB data, especially at higher energies after the peak. The magnitudes of the sums of the PICS calculated using both the MSD and the mBEB-B methods are lower than the TICS due to the lack of information on all the fragments and the AEs as our methods are dependent on the AEs and mass spectrum data of the fragments of the parent molecule.

The PICS of 2NI is shown in Figure. 7a, which contains the PICS of 8 fragments. The smallest fragment is $[HCNH]^+$ of m/z of 28 which has an AE of 11.44 eV and the biggest fragment is $[C_3H_3N_3O]^+$ having the m/z of 97. The $[C_3H_3N_2]^+$ cation has two AEs. Like the PICS of IMI a similar trend is seen here, both the MSD PICS and the mBEB-B PICS show a good agreement

TABLE II: Absolute values of branching ratio (Γ), structural factor (χ_i), scaling factor (Υ) and maximum PICS calculated using MSD and mBEB-B method compared with experimental PICS [36] for 2-butanol.

m/z	Cations ^a	ϵ (eV) [33]	Γ_i^H	Γ_i^{Theo}	Γ_i [33]	χ_i	Υ_i	σ_{max}^{MSD}	σ_{max}^{mBEB-B}	σ_{max}^{Exp} [36]
1	H	13.45	0.015970	0.826677	0.029448	1.843945	0.035623	0.328767	0.354294	0.0929
2	H_2	15.52	0.010394	0.662681	0.033981	3.269164	0.051278	0.374218	0.417960	0.0997
13	CH	15.38	0.010681	0.672343	0.033674	3.152747	0.050085	0.371191	0.413481	0.0254
14	CH_2	14.84	0.011890	0.711384	0.032492	2.732773	0.045674	0.359453	0.396460	0.1330
15	CH_3	9.99	0.038974	1.251373	0.021873	0.561216	0.017479	0.249473	0.257970	0.594
16	O/CH_4	13.3	0.016517	0.840578	0.02912	1.763079	0.034643	0.325416	0.349881	0.0459
17	OH	10.91	0.029923	1.113007	0.023887	0.798291	0.021462	0.270959	0.282552	0.0655
19	H_3O	13.56	0.015585	0.816679	0.029689	1.905022	0.036354	0.331219	0.357553	0.772
26	C_2H_2	11.5	0.025549	1.035467	0.025179	0.985502	0.024317	0.284586	0.298677	0.188
27	C_2H_3	13.87	0.014563	0.789364	0.030368	2.085312	0.038472	0.338110	0.366797	0.964
28	C_2H_4/CO	11.59	0.024959	1.024311	0.025376	1.016714	0.024774	0.286654	0.301163	0.279
29	C_2H_5/CHO	13.62	0.015380	0.811294	0.029821	1.939005	0.036757	0.332554	0.359333	0.834
30	CH_2O/C_2H_6	11.46	0.025818	1.040480	0.025091	0.971845	0.024115	0.283665	0.297576	0.0392
31	CH_3O	12.91	0.018059	0.878236	0.028266	1.565195	0.032185	0.316662	0.338509	1.27
32	CH_4O	12.5	0.019895	0.920350	0.027368	1.375620	0.029737	0.307408	0.326724	0.015
38	C_3H_2	13.11	0.017245	0.858645	0.028704	1.664470	0.033429	0.321159	0.344321	0.0289
39	C_3H_3	10.52	0.033375	1.168847	0.023033	0.690118	0.019706	0.261885	0.272052	0.198
40	C_2O/C_3H_4	10.35	0.035047	1.194444	0.022661	0.646585	0.018972	0.257912	0.267511	0.0317
41	C_2HO/C_3H_5	12.34	0.020679	0.937536	0.027018	1.306544	0.028818	0.303780	0.322175	0.801
42	C_2H_2O/C_3H_6	10.66	0.032078	1.148352	0.02334	0.727609	0.020325	0.265148	0.275806	0.0805
43	C_2H_3O/C_3H_7	11.77	0.023831	1.002498	0.02577	1.081357	0.025706	0.290782	0.306157	0.566
44	C_2H_4O/C_3H_8	10.35	0.035047	1.194444	0.022661	0.646585	0.018972	0.257912	0.267511	0.546
45	C_2H_5O	10.93	0.029759	1.110246	0.023931	0.804168	0.021555	0.271423	0.283094	2.53
46	C_2H_6O	10.67	0.031988	1.146908	0.023362	0.730346	0.020369	0.265381	0.276075	0.0629
51	C_4H_3	12.33	0.020729	0.938625	0.026996	1.302309	0.028761	0.303552	0.321891	0.0118
53	C_4H_5/C_3HO	12.01	0.022431	0.974409	0.026296	1.172314	0.026986	0.296266	0.312863	0.0198
54	C_4H_6/C_3H_2O	9.75	0.041924	1.291528	0.021347	0.509186	0.016529	0.243820	0.251661	0.0192
55	C_4H_7/C_3H_3O	12.34	0.020679	0.937536	0.027018	1.306544	0.028818	0.303780	0.322175	0.102
56	C_4H_8/C_3H_4O	9.45	0.046045	1.344407	0.020691	0.449368	0.01539	0.236726	0.243829	0.0483
57	C_3H_5O/C_4H_9	11.38	0.026366	1.050608	0.024916	0.944997	0.023716	0.281823	0.295374	0.0974
58	C_3H_6O	10.04	0.038395	1.243236	0.021982	0.572524	0.017682	0.250648	0.259290	0.0313
59	C_3H_7O	10.99	0.029274	1.102023	0.024062	0.821959	0.021835	0.272813	0.284722	0.84
60	C_3H_8O	10.66	0.032078	1.148352	0.02334	0.727609	0.020325	0.265148	0.275806	0.0298
72	C_4H_8O	9.66	0.043107	1.307068	0.02115	0.490645	0.016182	0.241695	0.249305	0.014
73	C_4H_9O	11.45	0.025886	1.041738	0.02507	0.968492	0.024065	0.283435	0.297300	0.0588
74	$C_4H_{10}O$	9.98	0.039092	1.253010	0.021851	0.558970	0.017439	0.249238	0.257706	0.0196
75	$^{13}C^{12}C_3H_{10}O$	9.79	0.041412	1.284707	0.021435	0.517603	0.016685	0.244764	0.252710	0.00111

^a The forward slash denotes "or" added for the cations with same m/z values

from the ionization threshold to 100 eV, after which the PICS of the MSD method falls short on comparison with the mBEB-B PICS, but their magnitudes remain similar.

The TICS of 2NI is shown in Figure. 7b, with the BEB model is compared with the TICS obtained after summing the cross sections of all the available fragments in the MSD and mBEB-B methods. The TICS do not match very well with the BEB TICS, as we don't have information on the AEs of all the fragments that appeared in the EIMS. All the details of the parameters required to compute PICS are given in the Table. IV, which contains the theoretical BRs, the experimental BRs, the scaling factors, and the structural factors along with the maximum CS.

IV. CONCLUSION

In the present work, we have theoretically computed the partial and total ionization cross sections of R-carvone, 2-butanol, imidazole, and 2-nitroimidazole using the MSD and mBEB-B methods in combination with the BEB model. We obtained a fairly good agreement of our theoretical PICS data of various fragments with the experimental PICS for R-carvone and 2-butanol. Also, the TICS which is obtained as the sum of all the PICS of the fragments in the MSD and mBEB-B method gives good agreement with TICS computed using the BEB model. For imidazole and 2-nitroimidazole, we could not find any experimental PICS study, and hence are computed in the present study for the first time. Hence, more investigation both theoretical and experimental is needed for these

TABLE III: Absolute values of branching ratio (Γ), structural factor (χ_i), scaling factor (Υ_i) and maximum PICS calculated using MSD and mBEB-B method compared for imidazole.

m/z	Cations	ε (eV) [40]	Γ_i^H	Γ_i^{Theo}	Γ_i [40]	χ_i	Υ_i	σ_{max}^{MSD}	σ_{max}^{mBEB-B}
28	<i>HCNH</i>	11.74	0.125833	0.700872	0.112307	0.892509	0.160239	1.043251	1.128965
40	<i>HCCNH</i>	14.96	0.060814	0.498982	0.246460	4.052667	0.493925	2.240973	2.592455
40	<i>HCNCH</i>	14.96	0.060814	0.498982	0.246460	4.052667	0.493925	2.240973	2.592455
41	<i>CH₂NCH</i>	11.68	0.127782	0.705604	0.025329	0.198219	0.035897	0.235377	0.254443
41	<i>CH₂CNH</i>	11.68	0.127782	0.705604	0.025329	0.198219	0.035897	0.235377	0.254443
41	<i>CHCHNH</i>	14.06	0.073256	0.546657	0.025329	0.345758	0.046334	0.231722	0.262657
67	<i>IMI-H</i>	8.76	0.302892	0.688466	0.007728	0.025516	0.054560	0.073110	0.378300

TABLE IV: Absolute values of branching ratio (Γ) structural factor (χ_i), scaling factor (Υ) and maximum PICS calculated using MSD and mBEB-B method compared for 2-nitroimidazole.

m/z	Cations	ε (eV) [40]	Γ_i^H	Γ_i^{Theo}	Γ_i	χ_i	Υ_i	σ_{max}^{MSD}	σ_{max}^{mBEB-B}
28	<i>HCNH</i>	11.44	0.124877	0.836333	0.112307	0.134285	0.134285	1.306890	1.388680
30	<i>NO</i>	11.11	0.136339	0.867858	0.070544	0.081285	0.081285	0.822306	0.868480
40	<i>HCCNH</i>	13.74	0.072078	0.654551	0.246460	0.376533	0.376533	2.832763	3.155850
56	<i>HNCHCO</i>	11.34	0.128210	0.845716	0.032927	0.038934	0.038934	0.383366	0.406602
67	<i>C₃H₃N₂</i>	13.00	0.085100	0.508922	0.037563	0.073808	0.073808	0.433492	0.475207
67	<i>C₃H₃N₂</i>	16.29	0.043251	0.508922	0.037563	0.073808	0.073808	0.425538	0.504195
83	<i>C₃H₃N₂O</i>	11.12	0.135971	0.866878	0.038764	0.044717	0.044717	0.451837	0.477295
97	<i>C₃H₃N₃O</i>	13.92	0.069318	0.642637	0.016542	0.025741	0.025741	0.189945	0.212466

molecules. The appearance energies and relative abundances of the fragments were the key parameters for the determination of the PICS, which were all taken from the experimental papers for our calculations. All other parameters such as the experimental and theoretical BRs, scaling factors, and structural factors employed for the determination of PICS were computed and are presented in Tables I, II, III and IV respectively. The TICS data obtained after summing all the PICS of the fragments in the MSD and mBEB-B method underestimates the TICS data computed using the BEB model for imidazole and 2-nitroimidazole. The discrepancy is due to the lack of complete information on the fragmentation of the parent molecule, where only the major dissociation fragments are given for imidazole and 2-nitroimidazole.

ACKNOWLEDGMENTS

S.S. acknowledges Vellore Institute of Technology for providing a research fellowship; D.G. acknowledges Science and Engineering Research Board (SERB), Department of Science and Technology (DST), Government of India (Grant No. SRG/2022/000394) for providing the

financial support and computational facility.

DATA AVAILABILITY STATEMENT

The data that support the findings of this study are available from the corresponding author upon reasonable request.

AUTHOR CONTRIBUTIONS

S. Suriyaprasanth: Conceptualization (lead), Data curation (lead), Investigation (lead), Methodology (Supporting), Resources (Supporting), Validation (lead), Writing – original draft (lead), Writing – review & editing (equal); **Rounak Agrawal:** Data curation (supporting), Methodology (Supporting), Investigation (Supporting); **Dhanoj Gupta:** Conceptualization (equal), Data curation (equal), Investigation (equal), Methodology (lead), Resources (lead), Validation (equal), Writing – original draft (equal), Writing – review & editing (lead), Supervision (lead).

- [1] Y. Itikawa, *Journal of Physical and Chemical Reference Data* **46**, 043103 (2017).
 [2] H.-T. Kim, J.-S. Lim, M.-S. Kim, H.-J. Oh, D.-H. Ko, G.-D. Kim, W.-G. Shin, and J.-G. Park, *Microelectronic*

Engineering **135**, 17 (2015).

- [3] B. Boudaïffa, P. Cloutier, D. Hunting, M. A. Huels, and L. Sanche, *Science* **287**, 1658 (2000).
 [4] L. Sanche, *Mass Spectrometry Reviews* **21**, 349 (2002).

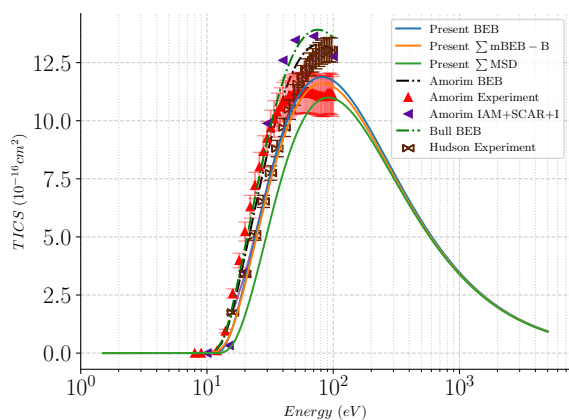


FIG. 4: Comparison of TICS of 2-butanol. The blue solid line represents the TICS calculated using the BEB method, the orange solid line represents the sum of all the PICS calculated by us using the mBEB-B method, the green solid lines represent the sum of all the PICS calculated by us using the MSD method. The back dashed-dotted lines represent the BEB TICS presented by Amorim *et al.*[36], the red upright triangle represents the experimental TICS presented by Amorim *et al.*[36] and their error bars are shown in pale pink colors, they have also provided the TICS calculated using the IAM+SCAR+I model which is shown by purple left triangle, the green dashed-dotted line represents the TICS presented by Bull *et al.*[53] and the brown bowtie represents the experimental TICS presented by Hudson *et al.*[54].

- [5] M. Rehman and E. Krishnakumar, *New Frontiers in Physical Science Research Vol. 2*, 102 (2022).
- [6] M. A. Rehman and E. Krishnakumar, *Atoms* **10**, 100 (2022).
- [7] D. Gupta and B. Antony, *The Journal of Chemical Physics* **141**, 054303 (2014).
- [8] D. Gupta, R. Naghma, and B. Antony, *Molecular Physics* **112**, 1201 (2014).
- [9] D. Gupta, H. Choi, S. Singh, P. Modak, B. Antony, D.-C. Kwon, M.-Y. Song, and J.-S. Yoon, *The Journal of Chemical Physics* **150**, 064313 (2019).
- [10] M. Vinodkumar, K. Joshipura, C. Limbachiya, and N. Mason, *Physical Review A* **74**, 022721 (2006).
- [11] A. Scheer, P. Mozejko, G. A. Gallup, and P. Burrow, *The Journal of chemical physics* **126**, 05B601 (2007).
- [12] V. Graves, B. Cooper, and J. Tennyson, *Journal of Physics B: Atomic, Molecular and Optical Physics* **54**, 235203 (2022).
- [13] K. Goswami, M. Luthra, A. K. Arora, A. Bharadvaja, and K. L. Baluja, *The European Physical Journal D* **76**, 97 (2022).
- [14] K. Boonruang, N. Kerddonfag, W. Chinsirikul, E. J. Mitcham, and V. Chonhenchob, *Food Control* **78**, 85 (2017).
- [15] M. Soleimani, A. Arzani, V. Arzani, and T. H. Roberts, *Journal of Herbal Medicine*, 100604 (2022).
- [16] D. Jones, E. Ali, C. Ning, F. Ferreira da Silva, O. Ingólfsson, M. Lopes, H. Chakraborty, D. H. Madison, and M. Brunger, *The Journal of Chemical Physics* **151** (2019).
- [17] M. Lopes, W. Pires, R. Amorim, A. Fernandes, T. Casagrande, D. Jones, F. Blanco, G. García, and M. Brunger, *International Journal of Mass Spectrometry* **456**, 116395 (2020).
- [18] R. Amorim, W. A. Pires, A. Fernandes, T. Casagrande, D. Jones, F. Blanco, G. García, M. Brunger, and M. Lopes, *The European Physical Journal D* **75**, 1 (2021).
- [19] R. Amorim, W. Pires, A. Fernandes, T. Casagrande, D. Jones, F. Blanco, G. García, M. Brunger, and M. Lopes, *International Journal of Mass Spectrometry* **464**, 116556 (2021).
- [20] P. J. Linstrom and W. G. Mallard, *Journal of Chemical & Engineering Data* **46**, 1059 (2001).
- [21] "Spectral database for organic compounds (sdfs)," .
- [22] F. Blanco and G. García, *Physics Letters A* **295**, 178 (2002).
- [23] F. Blanco and G. Garcia, *Physics Letters A* **317**, 458 (2003).
- [24] F. Blanco and G. García, *Physical Review A* **67**, 022701 (2003).
- [25] F. Blanco, L. Ellis-Gibbins, and G. García, *Chemical Physics Letters* **645**, 71 (2016).
- [26] L. Chiari, E. Anderson, W. Tattersall, J. Machacek, P. Palihawadana, C. Makochekekanwa, J. P. Sullivan, G. García, F. Blanco, R. McEachran, *et al.*, *The Journal of Chemical Physics* **138** (2013).
- [27] M. Iwahashi, M. Ikumi, H. Matsuzawa, Y. Moroi, M. A. Czarnecki, and Y. Ozaki, *Vibrational spectroscopy* **20**, 113 (1999).
- [28] M. C. A. Lopes, W. A. Pires, K. L. Nixon, R. A. Amorim, D. G. da Silva, A. C. Fernandes, S. Ghosh, D. B. Jones, L. Campbell, R. F. Neves, *et al.*, *The European Physical Journal D* **74**, 1 (2020).
- [29] W. Pires, K. Nixon, S. Ghosh, R. Amorim, R. Neves, H. V. Duque, D. da Silva, D. Jones, M. Brunger, and M. Lopes, *International Journal of Mass Spectrometry* **430**, 158 (2018).
- [30] S. Ghosh, K. Nixon, W. Pires, R. Amorim, R. Neves, H. V. Duque, D. da Silva, D. Jones, F. Blanco, G. Garcia, *et al.*, *International Journal of Mass Spectrometry* **430**, 44 (2018).
- [31] N. Bhavsar, T. Jani, P. Vinodkumar, C. Limbachiya, and M. Vinodkumar, *Radiation Physics and Chemistry* **202**, 110504 (2023).
- [32] H. Russmayer, H. Marx, and M. Sauer, *Biotechnology for biofuels* **12**, 1 (2019).
- [33] R. Amorim, A. Diniz, C. Oliveira, O. Oliveira Junior, D. Jones, F. Blanco, G. García, M. Brunger, and M. Lopes, *The European Physical Journal D* **76**, 207 (2022).
- [34] K. Nixon, W. Pires, R. Neves, H. V. Duque, D. Jones, M. Brunger, and M. Lopes, *International Journal of Mass Spectrometry* **404**, 48 (2016).
- [35] M. Bettiga, C. Winstead, and V. McKoy, *Physical Review A* **82**, 062709 (2010).
- [36] R. Amorim, C. Oliveira, O. Oliveira Junior, A. Diniz, D. Jones, J. Rosado, F. Blanco, G. García, M. Brunger, and M. Lopes, *The European Physical Journal D* **77**, 170 (2023).

- [37] R. Meissner, *Low-Energy Electron Interactions with Radiosensitisers and Hydrated Biomolecular Clusters*, Ph.D. thesis, Department of Physics of the Universidade Nova de Lisboa, Portugal (2019).
- [38] K. Shalini, P. K. Sharma, and N. Kumar, *Der Chemica Sinica* **1**, 36 (2010).
- [39] L. Zhang, X.-M. Peng, G. L. Damu, R.-X. Geng, and C.-H. Zhou, *Medicinal research reviews* **34**, 340 (2014).
- [40] R. Meissner, L. Feketeova, A. Ribar, K. Fink, P. Limão-Vieira, and S. Denifl, *Journal of The American Society for Mass Spectrometry* **30**, 2678 (2019).
- [41] T. Jani, P. Vinodkumar, and M. Vinodkumar, *The Journal of Physical Chemistry A* (2023).
- [42] Y.-K. Kim and M. E. Rudd, *Phys. Rev. A* **50**, 3954 (1994).
- [43] S. Suriyaprasanth, H. Choi, and D. Gupta, *Atoms* **11**, 137 (2023).
- [44] V. Vukstich, H. Bohachov, O. Vasiliev, and E. Y. Remeta, *Ukrainian Journal of Physics* **67**, 473 (2022).
- [45] M. Frisch, G. Trucks, H. Schlegel, G. Scuseria, M. Robb, J. Cheeseman, G. Scalmani, V. Barone, G. Petersson, H. Nakatsuji, *et al.*, *Wallingford CT* **421** (2016).
- [46] K. K. Irikura, *Journal of Research of the National Institute of Standards and Technology* **122**, 1 (2017).
- [47] J. R. Hamilton, J. Tennyson, S. Huang, and M. J. Kushner, *Plasma Sources Science and Technology* **26**, 065010 (2017).
- [48] S. E. Huber, A. Mauracher, D. Süß, I. Sukuba, J. Urban, D. Borodin, and M. Probst, *The Journal of Chemical Physics* **150**, 024306 (2019).
- [49] S. Grimme, *Angewandte Chemie International Edition* **52**, 6306 (2013).
- [50] J. Koopman and S. Grimme, *ACS omega* **4**, 15120 (2019).
- [51] K. Goswami, A. K. Arora, A. Bharadvaja, and K. L. Baluja, *The European Physical Journal D* **75**, 228 (2021).
- [52] R. Janev and D. Reiter, *Physics of Plasmas* **11**, 780 (2004).
- [53] J. N. Bull, P. W. Harland, and C. Vallance, *The Journal of Physical Chemistry A* **116**, 767 (2012).
- [54] J. E. Hudson, M. L. Hamilton, C. Vallance, and P. W. Harland, *Physical Chemistry Chemical Physics* **5**, 3162 (2003).

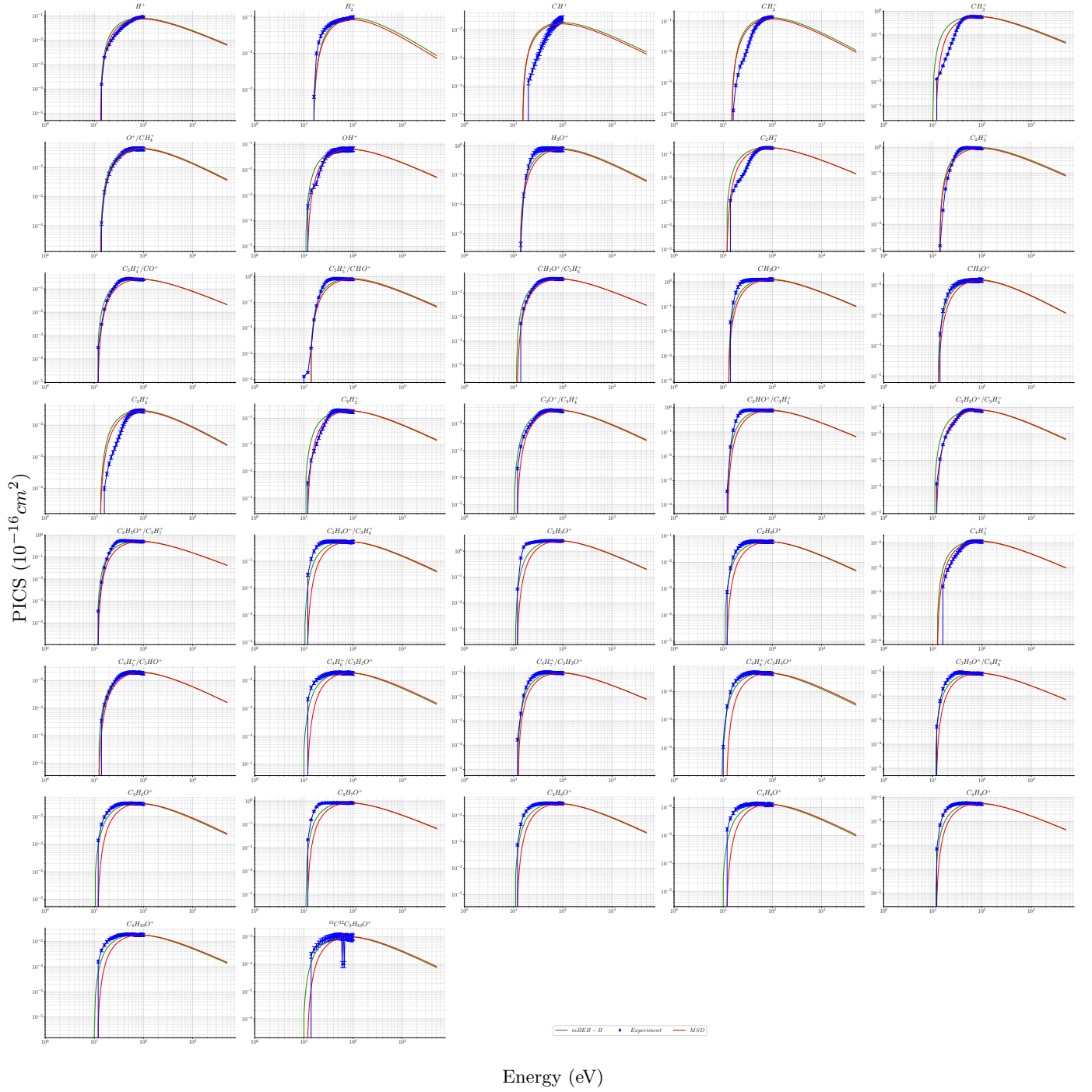
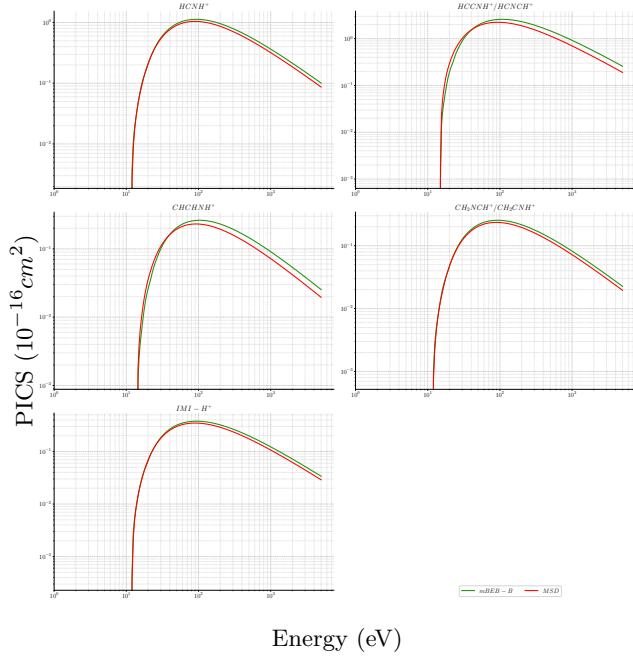
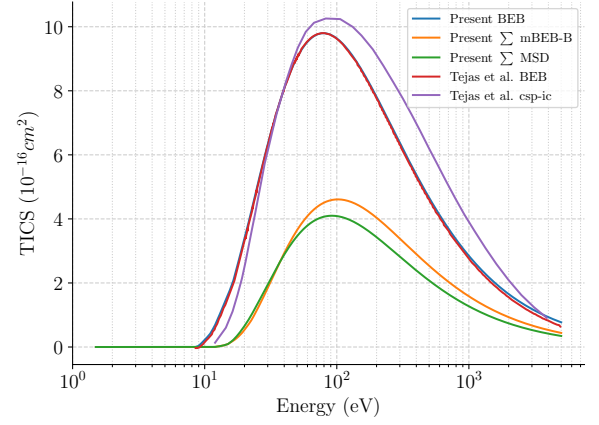


FIG. 5: Comparison of PICS calculated using various methods for 2-butanol. The X-axis represents the incident kinetic energy range in (eV), and the Y-axis represents the PICS in (10^{-16} cm^2). The green line represents the PICS calculated using the mBEB-B method, the red line represents the PICS calculated using the MSD method, and the blue Rhombus represents the experimental PICS presented by Amorim et al. [36], along with their error bars for each energy value.

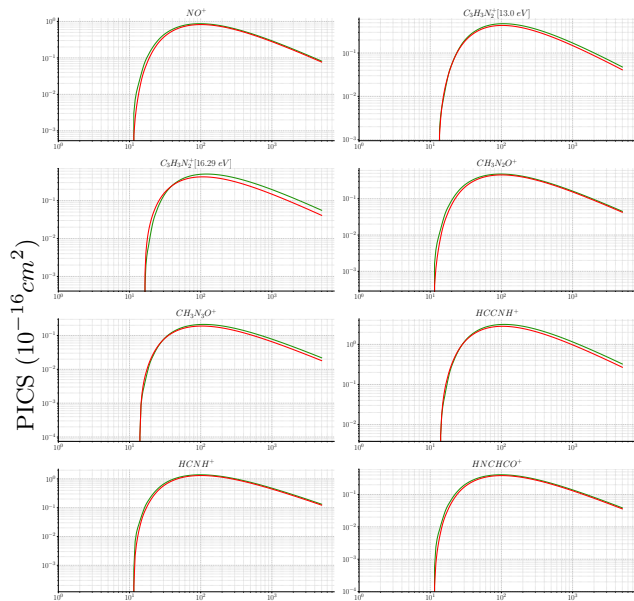


(a)

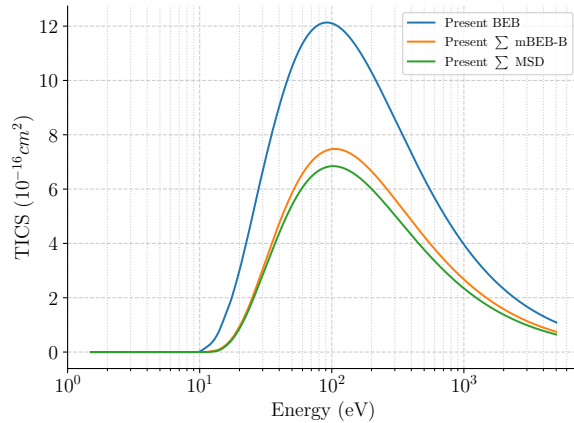


(b)

FIG. 6: a) Comparison of PICS calculated using various methods for imidazole. The green line represents the PICS calculated using the mBEB-B method, and the red line represents the PICS calculated using the MSD method, b) Comparison of TICS for imidazole, the blue line indicates the present BEB data, the orange line indicates the sum of PICS calculated using the mBEB-B method, the green line represents the sum of the PICS calculated using the MSD method, the red line, and the purple line represents the BEB TICS and the csp-ic TICS data presented by Tejas *et al.*[41].



(a)



(b)

FIG. 7: a) Comparison of PICS calculated using various methods for 2-nitroimidazole. The green line represents the PICS calculated using the mBEB-B method, and the red line represents the PICS calculated using the MSD method. b) Comparison of TICS for 2-nitroimidazole, the blue line presents our BEB-TICS, the green line shows the sum of PICS of MSD, and the orange line shows the sum of the PICS of the mBEB-B.